The American Journal of Pathology, Vol. 170, No. 2, February 2007

DOI: 10.2353/ajpath.2007.060505

Musculoskeletal Pathology

Oxidative Phenotype Protects Myofibers from Pathological Insults Induced by Chronic Heart Failure in Mice

Ping Li,* Richard E. Waters,* Shelley I. Redfern,* Mei Zhang,* Lan Mao,* Brian H. Annex,*† and Zhen Yan*

From the Department of Medicine, Duke University Medical Center, Durham; and the Department of Medicine,† Durham Veterans Administration, Durham, North Carolina*

The fiber specificity of skeletal muscle abnormalities in chronic heart failure (CHF) has not been defined. We show here that transgenic mice (8 weeks old) with cardiac-specific overexpression of calsequestrin developed CHF (50.9% decrease in fractional shortening and 56.4% increase in lung weight, $P < 0.001$), cachexia (37.8% decrease in body weight, $P < 0.001$), and exercise intolerance (69.3% decrease in running distance to exhaustion, $P < 0.001$) without a significant change in muscle fiber-type composition. Slow oxidative soleus muscle maintained muscle mass, whereas fast glycolytic tibialis anterior and plantaris muscles underwent atrophy (11.6 and 13.3%, respectively; $P < 0.05$). In plantaris muscle, glycolytic type IId/x and IIb, but not oxidative type I and IIa, fibers displayed significant decreases in cross-sectional area (20.3%, $P < 0.05$). Fast glycolytic white vastus lateralis muscle showed sarcomere degeneration and decreased cytochrome *c* oxidase IV (39.5%, $P < 0.01$) and peroxisome proliferator-activated receptor γ coactivator 1α protein expression (30.3%, $P < 0.01$) along with a dramatic induction of the *MAFbx/Atrogin-1* mRNA. These findings suggest that exercise intolerance can occur in CHF without fiber type switching in skeletal muscle and that oxidative phenotype renders myofibers resistant to pathological insults induced by CHF. ***(Am J Pathol 2007, 170:599–608; DOI: 10.2353/ajpath.2007.060505)***

It is well known that peripheral pathological changes in skeletal muscle figure prominently in the most prevalent clinical symptoms of chronic heart failure (CHF), exercise intolerance.[1–6] However, the structural complexity of skeletal muscle and the delicate relationship between skeletal muscle structure and function have impeded rapid progress of effective clinical intervention. Despite extensive research efforts and numerous reports in human patients and animal models of CHF on skeletal muscle abnormalities, including muscle wasting, decreased percentage of oxidative fibers, impaired excitation-contraction coupling, mitochondrial dysfunction, and vascular rarefaction,[4,7–12] the current understanding of muscle pathophysiology is still inadequate. Specifically, there is no information available regarding the fiber-type specificity of the abnormalities. Incomplete understanding of the etiology of CHF has undoubtedly hindered development of successful therapeutic regimens for this detrimental clinical symptom.

Results from many previous studies favor the hypothesis that exercise intolerance in CHF is attributable to specific myopathies characterized by atrophy and a shift from the slow-twitch fatigue-resistant oxidative fibers to the more fatigable fast-twitch glycolytic fibers.[7,13–15] However, recent studies have shown that improved exercise tolerance could occur without significant change in fiber-type composition in CHF patients,[16] supporting a view that slow-to-fast fiber-type switching does not solely account for exercise intolerance. Intriguingly, many studies have also shown that skeletal muscle rich in oxidative fibers are more resistant to and skeletal muscle rich in glycolytic fibers are more prone to metabolic abnormalities under pathological conditions.[17–23] These findings together illustrate a paradoxical paradigm and suggest the complexity in the development of this clinical symptom, which has prompted us to characterize the skeletal

Supported by the American Heart Association–Mid-Atlantic Affiliate (postdoctoral fellowship 0625518U to P.L., grant-in-aid 0555426U to Z.Y.) and the Veterans Administration Medical Center (merit review grant to B.H.A.).

Accepted for publication October 13, 2006.

Address reprint requests to Zhen Yan, Division of Cardiology, Department of Medicine, Duke University Medical Center, 4321 Medical Park Dr., Suite 200, Durham, NC 27704; or Brian H. Annex, Division of Cardiology, Department of Medicine, Durham, VA and Duke University Medical Center, 508 Foulton St., Durham, NC 27705. E-mail: zhen.yan@duke.edu and annex001@mc.duke.edu.

muscle abnormalities more comprehensively in a genetic mouse model of CHF. An improved understanding of the pathological changes in peripheral skeletal muscle under the CHF condition will help develop effective therapeutics for this clinical etiology.

In this study, we took advantage of our newly developed fiber type-specific analyses to ascertain whether CHF results in skeletal muscle abnormalities in a fiber type-specific manner. We hypothesized that glycolytic fibers are more susceptible than oxidative fibers to the pathological insults induced by CHF. We showed that exercise intolerance can occur without a significant change in skeletal muscle fiber type composition in mice with CHF. We have also obtained comprehensive morphological, biochemical, and gene expression evidence to indicate that multiple skeletal muscle abnormalities, including vascular rarefaction, reduced mitochondrial oxidative enzyme expression, myopathy, and muscle atrophy, are all manifested in glycolytic fibers, consistent with a notion that oxidative muscle phenotype is associated with a protective mechanism against the pathological insults caused by CHF.

Materials and Methods

Experimental Animals

Transgenic mice (DBA/C57BL/6, 8 weeks old) with cardiac-specific overexpression of the sarcoplasmic reticulum Ca^{2+} storage protein calsequestrin (CSQ)[24,25] and the wild-type (WT) littermates were housed in temperature-controlled quarters (21°C) with 12-hour light/dark cycles and provided with water and chow (Purina, Richmond, IN) *ad libitum*. The hindlimb muscles, lung, and heart were harvested after the mice were sacrificed by an intraperitoneal overdose injection of sodium pentobarbital (125 mg/kg, i.p.); organs were measured for wet weight and processed for further analyses. All animal protocols were approved by the Duke University Institutional Animal Care and Use Committee.

Transthoracic Echocardiography

Two-dimensional guided M-mode and Doppler echocardiography was performed using an HDI 5000 echocardiograph (ATL, Bothell, WA) in conscious mice as described previously.[26,27] Three independent echocardiographic measurements were taken in both modes for each mouse for the following parameters: left ventricular end-diastolic dimension (LVEDD) and left ventricular end-systolic dimension (LVESD) to obtain a mean value. Left ventricular fraction shortening (FS%) was calculated as FS% = (LVEDD − LVESD)/LVEDD × 100%.

Determination of Exercise Intolerance

The mice were housed in a designated treadmill test room with dark-light cycle control (3:00 PM off, 3:00 AM on) for 3 days. They were then subjected to running on a 16-track motorized treadmill at a low speed (0.5 mph, 0% incline) for 10 minutes each day for 3 days to be acclimatized to treadmill running. The acclimatization sessions always started at 5 minutes after the start of the dark cycle. These pretest training sessions are considered essential to minimize variability of the running test results. On day 4, food was removed 3 hours before the dark cycle, and mice were tested on the treadmill beginning with a parameter of 0.5 mph and 5% incline. The speed was increased by 0.1 mph every 30 minutes up to 1 mph. To ensure humane treatment of the animals, mice were encouraged to run by being stimulated on the tail with a soft brush attached to the back door that could be easily opened. Exhaustion was defined as mice that refused to run for 10 seconds. The custom-designed back door of the running track chamber was then opened immediately to terminate the test. The time of running for each mouse was recorded, and the total distance was calculated. To minimize subjectivity of the tests, the person who was responsible for the treadmill test was unaware of the genotype of the mice. To exclude the possibility that treadmill running induces damage and acute responses in recruited skeletal muscles that could confound the analyses, we performed the treadmill running test for a different set of mice from the ones we performed comprehensive morphological, biochemical, and gene expression analyses.

Determination of Skeletal Muscle Fiber Type Composition

Fiber type composition was determined in plantaris muscles as described previously.[28] In brief, isolated muscles were immersed in 30% sucrose/phosphate-buffered saline solution (PBS) for ~2 hours at 4°C and frozen in liquid nitrogen-cooled isopentane. Frozen sections (5 μm) were cut and fixed in 4% paraformaldehyde/PBS for 10 minutes and permeabilized with 0.3% Triton X-100/PBS for 10 minutes at 4°C. The sections were then blocked by 5% normal goat serum (NGS)/PBS for 30 minutes at room temperature, followed by incubation with mouse anti-myosin heavy chain I (MHC I) (BA-F8, 1:25; German Collection of Microorganisms and Cell Cultures) and rat anti-laminin (MAB1928, 1:100; Chemicon, Temecula, CA) in 5% NGS/PBS overnight at 4°C. After washing in PBS, the sections were then incubated with fluorescein-conjugated goat anti-rat IgG (1:25) and cyanine Cy5-conjugated mouse IgG (1:25) in 5% NGS/PBS for 30 minutes at room temperature. The sections were then washed three times with PBS, fixed in 4% paraformaldehyde for 2 minutes at 4°C, and blocked with 5% NGS/PBS for 30 minutes. Sequential incubations as described above were then performed with MHC IIa antibody (SC-71, 1:100; German Collection of Microorganisms and Cell Cultures) and rhodamine red-X-conjugated goat anti-mouse IgG. (1:25). Digital images were captured under a confocal microscope (Olympus). Type I (Cy5-labeled), type IIa (rhodamine red-X-labeled) and type IId/x + IIb (unstained) fibers were counted for the whole section, and each type was presented as percentage of the total fibers. To assess the degree of muscle wasting, we used Scion Image software (Scion, Frederick, MD) to measure

the cross-sectional area for the plantaris muscles and the cross-sectional area for type I, IIa, and IId/x + IIb fibers based on the fiber boundary stained positive for laminin (all type I and IIa fibers, and $n > 30$ of type IId/x + IIb fibers).

Determination of Capillary Density

Similar procedures were followed as described above except that different primary and secondary antibodies were used: mouse anti-dystrophin (D8043, 1:100; Sigma, St. Louis, MO) and rat anti-CD31 (MCA1364, 1:25; Serotec, Raleigh, NC) followed by fluorescein-conjugated goat anti-rat IgG (1:25) and cyanine Cy5-conjugated goat anti-mouse IgG (1:25). To determine capillarity, three complementary quantification approaches were taken. First, we counted total number of capillaries (fluorescein-labeled) on the entire cross-section for each muscle and presented as capillaries per unit area. Second, we obtained capillary-to-fiber ratio by dividing the number of capillaries by the number of muscle fibers to account for increased capillary density per unit area attributable to myofiber atrophy. Third, we determined fiber type-specific capillary contacting, ie, the number of capillaries in contact with a muscle fiber. This analysis provides evidence of fiber type specificity of vascular rarefaction. Capillaries in contact with type IIa and IId/x + IIb fibers were counted (total >50 fibers were counted for each type). Because only a very small proportion of myofibers were type I fibers in plantaris muscle (Table 2), capillary contacting for type I fibers were not included in the analysis.

Transmission Electron Microscopy

Transmission electron microscopy analysis was perform at Duke Electron Microscopy Service for soleus and white vastus lateralis muscle longitudinal sections from CSQ and WT mice ($n = 2$ for each genotype, 10 weeks of age in DBA background) according to the method described previously.[29] Sarcomere length and *Z* line thickness were measured (124 to 194 sarcomeres and 12 to 14 *Z* lines were measured for each muscle and genotype).

Atrophic Response in Skeletal Muscle in Vivo

To test further if there is a differential induction of *MAFbx/Atrogin-1* and *MuRF1* between slow oxidative and fast glycolytic muscles in response to atrophic stimuli, WT C57BL/6 mice (8 to 9 weeks old) were intraperitoneally injected with lipopolysaccharide (LPS; 1 mg/kg) or tumor necrosis factor-α (TNF-α; 0.1 mg/kg). Mice injected with normal saline served as control. Twelve hours (for LPS) or eight hours (for TNF-α) after injection, soleus and white vastus lateralis muscles were harvested for analysis of *MAFbx/Atrogin-1* and *MuRF1* mRNA expression by semiquantitative reverse transcriptase-polymerase chain reaction (RT-PCR) as described next.

Semiquantitative RT-PCR

This analysis was performed as described[30] to measure endogenous *MAFbx/Atrogin-1* and *MuRF1* mRNA expression in soleus and white vastus lateralis muscles in CSQ and WT mice. PCR primer pairs were designed using Primer3 search engine at *http://www-genome.wi.mit.edu*. The oligonucleotide primer pairs used for these genes in this study corresponded to the following nucleotides: *MAFbx/Atrogin-1*: 1917 to 1936 and 2415 to 2396 (NM_026346); and *MuRF1*: 50 to 69 and 452 to 433 (AF294790). Results were normalized by housekeeping gene cyclophilin mRNA[31] or 18S rRNA[28] and presented as fold change to soleus muscle in WT mice.

Western Immunoblot Analysis

For protein analysis, dissected muscles were homogenized and analyzed as described previously.[28] The following antibodies were used for immunoblot analysis: α-tubulin antibody (13-8000; Zymed, South San Francisco, CA), cytochrome *c* oxidase IV (COXIV) (A-21348; Molecular Probes, Eugene, OR), peroxisome proliferator-activated receptor γ co-activator 1α (PGC-1α) (SC-13067; Santa Cruz Biotechnology, Santa Cruz, CA), and MHCs (BF-F8 for MHC I, SC-71 for MHC IIa, and BF-F3 for MHC IIb; German Collection of Microorganisms and Cell Cultures). The intensities of the bands were quantified by using Scion Image software and normalized by α-tubulin.

Statistics

Data are presented as mean ± SE. For comparisons involving two factors, eg, genotype and gender, two-way analysis of variance was performed followed by the Newman-Keuls test. For comparisons between two groups, the Student's *t*-test was performed. Paired *t*-test was performed for comparisons between white vastus lateralis and soleus muscles in the same mouse after LPS or TNF-α injection. $P < 0.05$ was accepted as statistically significant for all of the experiments in this study.

Results

Cardiac-Specific Overexpression of CSQ Induces Heart Failure, Cardiac Cachexia, and Exercise Intolerance in Mice

Consistent with the previous reports,[25,32] male CSQ mice (8 weeks of age in DBA/C57BL/6 background) developed severe cardiac hypertrophy as shown by a profound increase (approximately threefold) in biventricular heart weight (Figure 1A). No significant difference in tibia length was observed between WT and CSQ mice (17.2 ± 0.2 mm in CSQ mice versus 16.9 ± 0.3 mm in WT mice, $P > 0.05$), indicating that CSQ mice did not suffer from growth retardation. CSQ mice had severely compromised cardiac function as shown by significantly de-

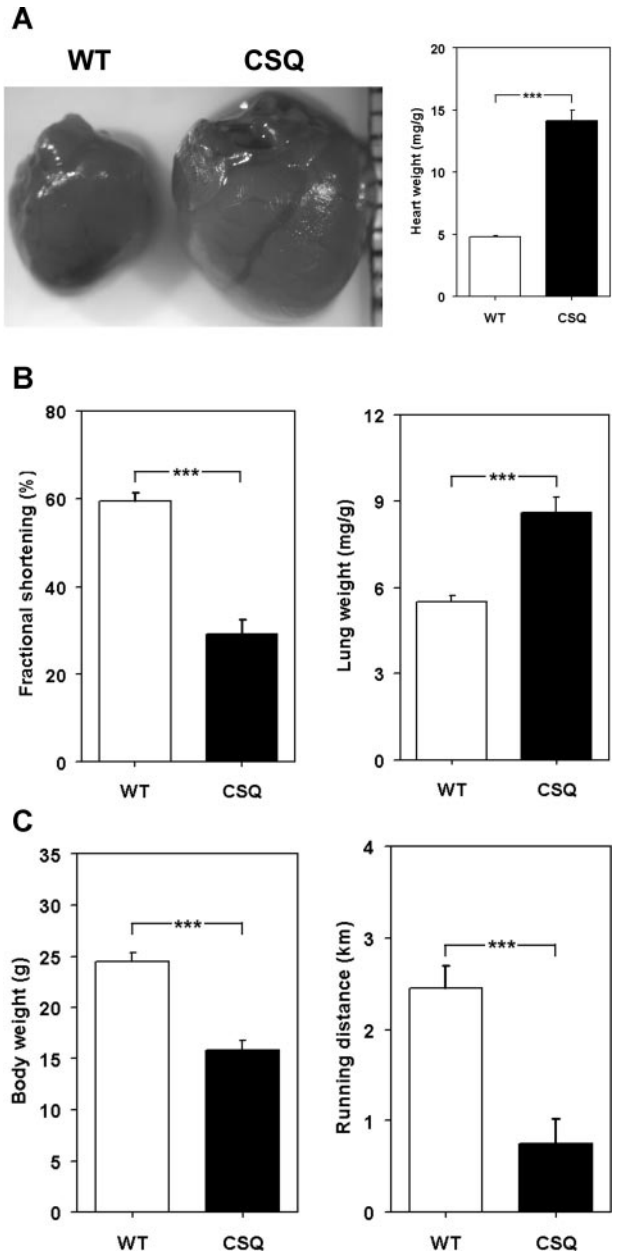

Figure 1. CHF leads to cachexia and exercise intolerance in mice. **A:** An image of hearts from WT and CSQ mice showing cardiac hypertrophy in CSQ mice (left) as reflected by a significant increase in the heart weight normalized by body weight (right). **B:** Fractional shortening and lung weight in WT and CSQ mice. **C:** Body weight and treadmill running distance to exhaustion in WT and CSQ mice. $^{***}P < 0.001$, $n = 5$ to 7.

creased fractional shortening (50.9%, $P < 0.001$) based on echocardiograph analysis and by increased lung weight (57.7%, $P < 0.001$) compared with WT mice (Figure 1B). CSQ mice also developed severe cachexia as shown by a significant decrease in body weight compared with WT mice (37.8%, $P < 0.001$) (Figure 1C). To determine whether CSQ mice developed exercise intolerance, we performed a treadmill running test for CSQ and WT mice. The running distance to exhaustion in CSQ mice was significantly reduced (2.4 ± 0.2 km versus 0.7 ± 0.3 km in WT mice, $P < 0.001$) (Figure 1C). Female mice at the same age showed a similar approximately

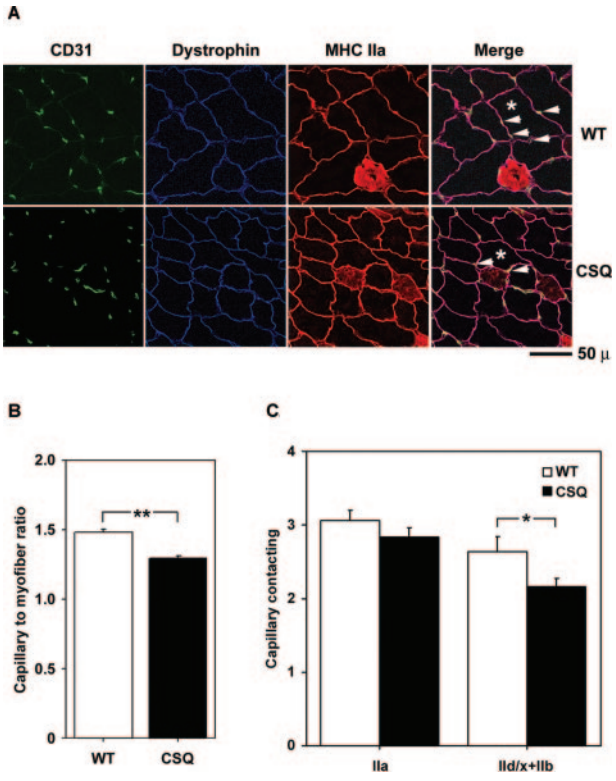

Figure 2. CHF results in vascular rarefaction in fast glycolytic fibers in mice. **A:** Indirect immunofluorescence staining for CD31 (green), dystrophin (blue), and MHC IIa (red) in plantaris muscles of CSQ and WT mice with merged images (merge). **Arrows** point to endothelial cells positive for CD31 around a type IId/x + IIb fiber (*). A decreased capillary contacting in CSQ sample could be appreciated. **B:** Capillary to myofiber ratio in plantaris muscles. **C:** Capillary contacting in type IIa and IId/x + IIb myofibers. Bars represent means ± SE ($n = 5$). $^{*}P < 0.05$ and $^{**}P < 0.01$.

threefold increase in heart weight (4.6 ± 0.1 mg/g body weight in WT versus 13.0 ± 0.9 mg/g body weight in CSQ mice, $P < 0.001$); however, they did not display any significant changes in body, lung, and skeletal muscle weight as well as other parameters that we measured later in the study, such as capillary density, myofiber size, and fiber type composition in plantaris muscle (not shown). Because we could not definitively determine whether lack of whole body cachexia and muscle abnormalities was attributable to lack of heart failure or a gender difference, we did not include female mice in the later analyses, leaving the gender difference to future studies.

Vascular Rarefaction Is Prevalent in Fast-Twitch, Glycolytic Fibers in CSQ Mice

To determine whether heart failure results in vascular rarefaction in a fiber type-specific manner, we performed indirect immunofluorescence using antibodies against MHC IIa, dystrophin, and CD31 for plantaris muscle cross-sections (predominantly glycolytic type IId/x and IIb fibers and some oxidative type I and IIa fibers) from CSQ and WT mice (Figure 2A). Capillary to fiber ratio was significantly decreased (12.8%, $P < 0.01$) in CSQ mice compared with WT mice (Figure 2B). Further analysis by counting capillaries in contact with individual myofibers

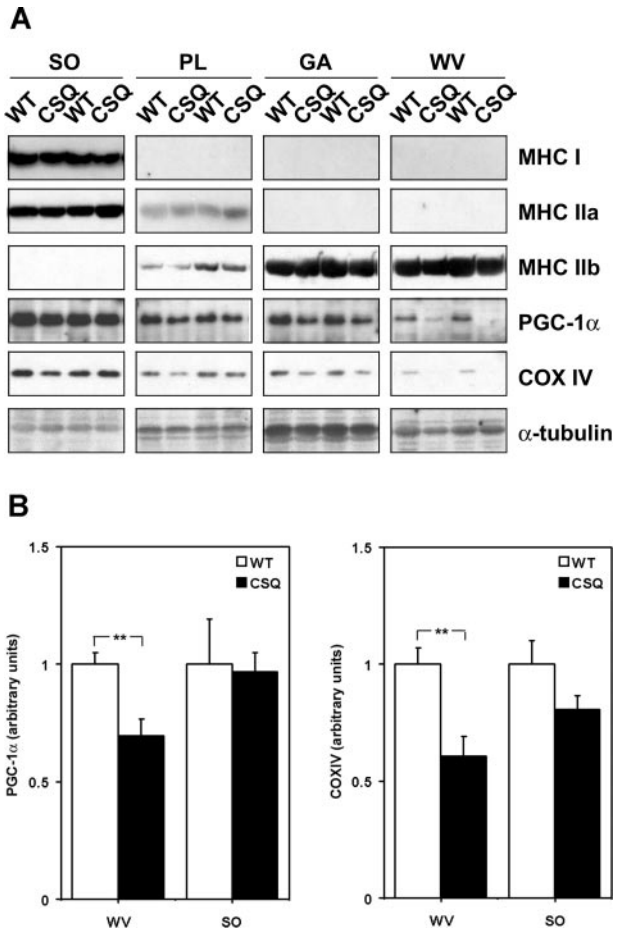

Figure 3. CHF results in decreased mitochondrial oxidative enzyme in fast glycolytic muscles. **A:** Representative images of Western blot analysis for MHC isoforms, PGC-1α, COX IV proteins with α-tubulin as loading control in soleus (SO), plantaris (PL), gastrocnemius (GA), and white vastus lateralis (WV) muscles in CSQ and WT mice. **B:** Comparison of COXIV and PGC-1α protein expression in WV and SO muscles between WT and CSQ mice (n = 5 to 6). Bars represent means ± SE. $^{**}P < 0.01$.

showed a significant decrease in capillary contacting in glycolytic fibers (18.2%, $P < 0.05$) but not around oxidative type IIa fibers in CSQ mice (Figure 2C).

Mitochondrial Oxidative Enzyme Expression Decreases in Fast-Twitch, Glycolytic Muscles in CSQ Mice

To characterize the skeletal muscle abnormalities with regard to the expression of contractile protein isoforms and mitochondrial biogenesis, we performed Western immunoblot analysis for MHC isoforms (I, IIa, and IIb), COXIV, and PGC-1α proteins in skeletal muscles of different fiber type compositions. MHC protein expression was not significantly different between CSQ and WT mice in four different hindlimb muscles. White vastus lateralis muscle in CSQ mice showed significantly decreased COX IV (39.5%, $P < 0.01$) and PGC-1α protein expression (30.3%, $P < 0.01$) compared with WT mice (Figure 3, A and B). A similar trend (not statistically significant) of decreased COXIV and PGC-1α protein expression was noticed in gastrocnemius (predominantly glycolytic type IId/x and IIb fibers and some oxidative type I and IIa fibers) and plantaris muscles, whereas no differences were observed in soleus muscle (Figure 3, A and B).

Table 1. Comparison of Muscle Weight and Plantaris Muscle Fiber Type Composition between CSQ and WT Mice

	WT	CSQ
Muscle weight	$n = 6$	$n = 5$
Tibialis anterior	1.75 ± 0.04	1.57 ± 0.05*
Plantaris	0.60 ± 0.01	0.53 ± 0.03*
Soleus	0.29 ± 0.01	0.31 ± 0.01
Fiber type	$n = 5$	$n = 6$
Type I (%)	0.8 ± 0.4	1.2 ± 0.4
Type IIa (%)	28.2 ± 2.3	30.2 ± 2.4
Type IIb + IId/x (%)	71.0 ± 2.1	68.6 ± 2.6

Values are means ± SE.
*$P < 0.05$.

Fast-Twitch, Glycolytic Fibers Undergo Atrophy and Sarcomere Degeneration in CSQ Mice

To characterize the fiber type specificity of muscle atrophy, we measured muscle weight for several hindlimb muscles and observed a significant decrease in muscle weight (normalized by body weight) in tibialis anterior (11.6%, $P < 0.05$) (predominantly glycolytic type IId/x and IIb fibers and some oxidative type I and IIa fibers) and plantaris muscles (13.3%, $P < 0.05$) in CSQ mice compared with WT mice (Table 1). No significant loss of muscle mass was observed in soleus muscle when normalized by body weight. Using indirect immunofluorescence with antibodies specific for MHC isoforms,[33] we confirmed that there were no significant differences in fiber type composition in plantaris muscles between CSQ and WT mice (Table 1), consistent with the Western blot findings (Figure 3, A and B). To further determine the fiber type specificity of myofiber atrophy, we measured the cross-sectional areas for the whole plantaris muscle as well as individual myofibers of different fiber types in plantaris muscle (Figure 4A). The cross-sectional area of plantaris muscle in CSQ mice decreased significantly (39.5%, $P < 0.05$), which was also reflected by an increased fiber number per unit area (31.8%, $P < 0.05$) (Figure 4B). Fiber type-specific analysis for individual fibers in plantaris muscle revealed a significant decrease of cross-sectional area in glycolytic type IId/x + IIb fibers (20.3%, $P < 0.05$) and a trend of decrease in oxidative type IIa fibers (15.1%, $P = 0.13$), but not in oxidative type I fibers (Figure 4, C and D). To further characterize the pathological changes in skeletal muscles of CSQ mice, we performed transmission electron microscopy analysis. As shown (Figure 4, E and F), compared with WT mice, soleus muscle (predominantly oxidative type I and IIa fibers) in CSQ mice displayed relatively normal structural features of the *Z* line and good alignment of sarcomeres. However, in white vastus lateralis muscle (nearly 100% glycolytic type IIb fibers) of CSQ mice, both the *Z* and *M* lines appeared paler, thinner, and more curved

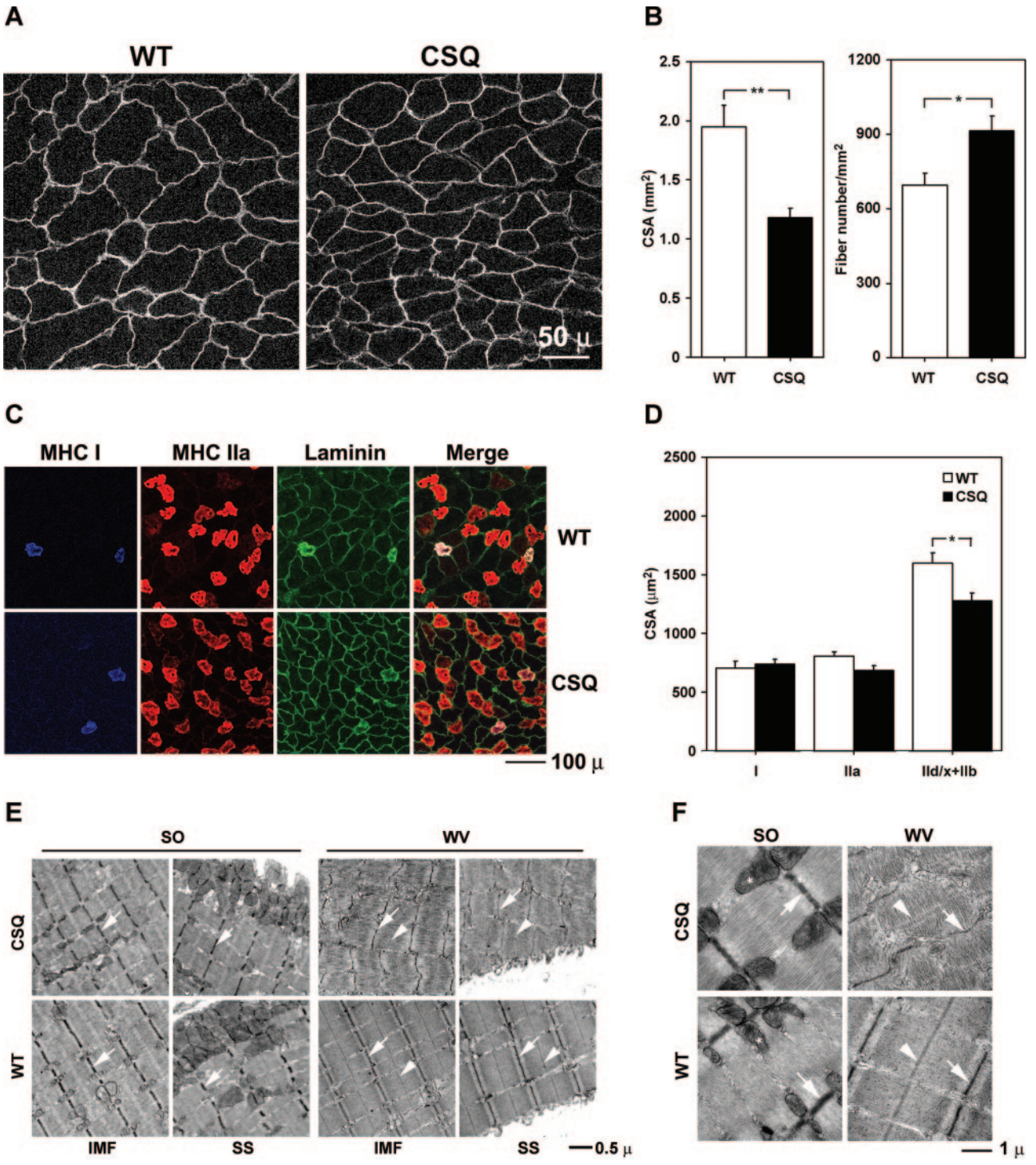

Figure 4. CHF induces manifested atrophy and sarcomere degeneration in fast glycolytic fibers. **A:** Representative images of indirect immunofluorescence staining for dystrophin in plantaris muscle cross-sections from CSQ and WT mice. **B:** Plantaris muscle cross-sectional area (CSA) and fiber number per unit area (mm^2) in CSQ and WT mice ($n = 5$). **C:** Indirect immunofluorescence staining of MHC I (blue), MHC IIa (red), and laminin (green) and merged images (merge) in plantaris muscles from CSQ and WT mice. A cross-reactivity of fluorescein-conjugated goat anti-rat IgG against MHC I was noted, but it did affect the analysis. A decreased myofiber cross-sectional area for type IId/x + IIb (negative cytosolic staining) fibers can be appreciated. **D:** Cross-sectional area for type I, IIa, and IId/x + IIb myofibers in plantaris muscles of CSQ and WT mice ($n = 5$). Bars are presented as means ± SE. * and ** denote a statistical differences with $P < 0.05$ and 0.01, respectively, compared with WT mice. **E:** Transmission electron microscopy analysis for soleus (SO) and white vastus lateralis (WV) muscles from CSQ and WT mice at the subsarcolemmal (SS) and intermyofibrillar areas (IMF). The *Z* (**arrows**) and *M* lines (**arrowheads**) became thin and curved, the sarcomeres were shortened and disarrayed in WV muscle of CSQ mice compared with WT mice, but the structural features of the sarcomeres remained relatively normal in SO muscle from the same mouse. **F:** Transmission electron microscopy analysis for soleus (SO) and white vastus lateralis (WV) muscles from CSQ and WT mice. The high-magnification image showed that the mitochondrial structures (*) in soleus muscle, such as inner and outer membranes and cristae, were preserved well in CSQ mice. Likewise, the *Z* (**arrows**) and *M* lines (**arrowheads**) were thin and curved, and the sarcomeres were shortened and disarrayed in WV muscle of CSQ mice but less so in SO muscle from the same mouse (please refer to Table 2). It could be clearly appreciated that the thick filaments were out of register in WV muscle from CSQ mice. Original magnifications: ×5000 (**E**); ×22,000 (**F**).

Table 2. Comparison of Sarcomere Length and *Z* Line Thickness between CSQ and WT Mice

	SO			WV		
	WT	CSQ	% change	WT	CSQ	% change
Sarcomere length (μm)	1.67 ± 0.01 (124)	1.36 ± 0.01*** (151)	−19.0	1.87 ± 0.00 (132)	1.38 ± 0.01*** (194)	−26.5
Z line thickness (nm)	124.2 ± 2.5 (12)	114.6 ± 3.0* (14)	−7.7	59.0 ± 1.8 (13)	48.6 ± 2.1*** (12)	−17.6

Values are means ± SE (number of measurements).
*$P < 0.05$.
***$P < 0.001$.

than those in the WT mice, and the sarcomeres were disarrayed (Figure 4, E and F). White vastus lateralis muscle in CSQ mice had more profound decreases in both sarcomere length (19.0% in soleus versus 26.5% in white vastus lateralis) and *Z* line thickness (7.7% in soleus versus 17.6% in white vastus lateralis) than soleus muscle (Table 2). These structural changes were detected both at the subsarcolemmal and intermyofibrillar areas in CSQ mice (Figure 4F). Mitochondrial structure was generally preserved in soleus muscle from CSQ mice compared with that from WT mice (Figure 4F).

CHF Results in a Significant Induction of MAFbx/Atrogin-1 mRNA Expression in Fast Glycolytic Muscle

To obtain further evidence at the gene transcription level that support the findings of fiber type-specific muscle wasting, we measured *MAFbx/Atrogin-1* and *MuRF1* mRNA expression in soleus and white vastus lateralis muscles in CSQ and WT mice. The *MAFbx/Atrogin-1* and *MuRF1* genes encode striated muscle-specific E3 ligases functioning in the proteosome-dependent protein degradation pathway for muscle catabolism.[34,35] Soleus muscle in CSQ mice showed a trend of increase (not statistically significant), but white vastus lateralis muscle showed a very dramatic increase ($P < 0.001$) in *MAFbx/Atrogin-1* mRNA expression compared with WT mice (Figure 5, A and B). Interestingly, unlike other types of muscle atrophy,[36] there was no induction of *MuRF1* mRNA in either soleus or white vastus lateralis muscles in CSQ muscle. To determine whether this finding could be generalized to other experimental conditions of skeletal muscle wasting,[37–40] we measured *MAFbx/Atrogin-1* and *MuRF1* mRNA in white vastus lateralis and soleus muscles *in vivo* after intraperitoneal injection of LPS or TNF-α. Consistent with the notion that slow oxidative muscles are more resistant to atrophic stimuli, we found more dramatic induction of *Atrogin-1* mRNA in white vastus lateralis muscle than in soleus muscle after either LPS or TNF-α injection, and *MuRF1* mRNA was not induced in soleus muscle at all but was significantly increased in white vastus lateralis muscle.

Discussion

Many studies have reported skeletal muscle abnormalities in human patients and animal models of CHF[1–6]; however, the pathological changes remain incompletely defined. Specifically, there is no information available regarding the fiber type specificity. Here, in a mouse genetic model of CHF, we have obtained evidence of manifested vascular rarefaction, reduction of mitochondrial oxidative enzyme expression, muscle atrophy, and enhanced E3 ligase *MAFbx/Atrogin* gene expression in fast-twitch, glycolytic fibers, whereas slow-twitch, oxidative fibers are relatively spared of these abnormalities. Therefore, our findings provide comprehensive morphological, biochemical, and gene expression evidence supporting the view that oxidative muscle phenotype is associated with a protective mechanism against the pathological insults caused by CHF. This type of CHF-induced muscle atrophy is associated with enhanced expression of muscle-specific E3 ubiquitin ligase *MAFbx/Atrogin-1* mRNA, but not *MuRF1* mRNA. Our data also show that exercise intolerance can be induced in an animal model of CHF without a significant change in fiber type composition in skeletal muscle.

It has been demonstrated that vascular rarefaction is associated with skeletal muscle dysfunction in CHF[41,42]; however, there has been no formal report on fiber type specificity of vascular rarefaction in skeletal muscle in CHF. Our simultaneous immunofluorescence staining for MHC isoforms and endothelial cell marker CD31 revealed decreased capillary contacting in glycolytic type IId/x + IIb fibers, not in oxidative type IIa fibers (Figure 2C), providing direct evidence that decreased capillary density occurs in a fiber type-specific manner as well. It is worthy to note that because of myofiber atrophy there was actually a trend of increased capillary density per unit area in skeletal muscle of CSQ mice (not shown). This trend in capillary density may serve as a compensatory mechanism to maintain the supply of oxygen and nutrients under the disease condition.

A decline in mitochondrial number and function has been offered as an explanation for the rapid development of muscle fatigue during exercise,[43,44] which is strongly supported by the findings that mitochondrial volume density correlates closely with exercise capacity in different patients and in the same patients throughout time.[4] Impaired mitochondrial biogenesis/function is likely to play a role in initiating the pathological changes attributable to enhanced production of reactive oxygen species and/or reduced anti-oxidant capacity. A fiber type-specific impairment of mitochondrial morphology and function has not been reported in skeletal muscles in human patients with CHF because of fiber type heterogeneity and limitation of the available techniques. Here, we obtained clear evidence in CSQ mice that mitochondrial oxidative enzyme expression decreases in skeletal muscles rich in fast-twitch, glycolytic fibers. It remains to be determined

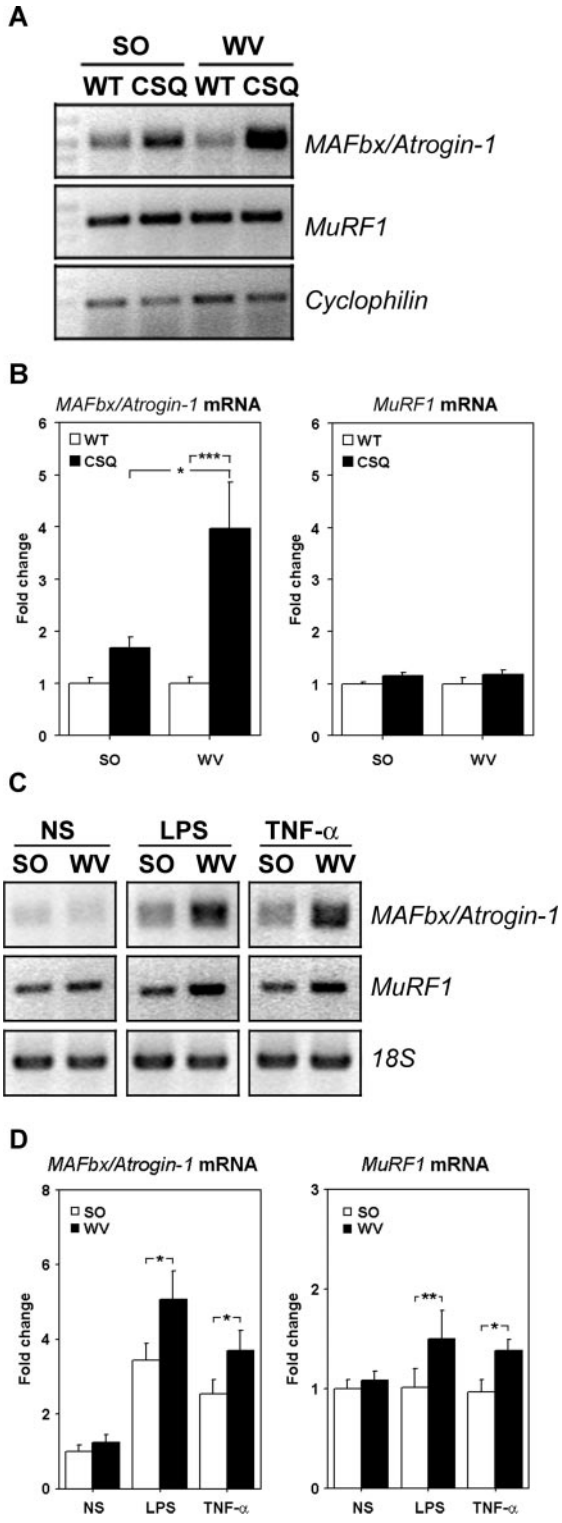

Figure 5. CHF results in a more dramatic induction of *MAFbx/Atrogin-1* mRNA, but not *MuRF1* mRNA, in fast glycolytic muscle than slow oxidative muscle. **A:** Representative DNA gel images for semiquantitative RT-PCR analysis for *MAFbx/Atrogin-1* and *MuRF1* mRNA with cyclophilin as control for total RNA quantity and quality in white vastus lateralis (WV) and soleus (SO) muscles in WT and CSQ mice. **B:** Quantitative data for *MAFbx/Atrogin-1* and *MuRF1* mRNA ($n = 6$). * and *** denote $P < 0.05$ and 0.001, respectively. **C:** Representative DNA gel images for semiquantitative RT-PCR analysis for *MAFbx/Atrogin-1* and *MuRF1* mRNA with 18S rRNA as control for total RNA quantity and quality in WV and SO muscle after TNF-α or LPS injections. **D:** Quantitative data for *MAFbx/Atrogin-1* and *MuRF1* mRNA ($n = 5$). *$P < 0.05$ and **$P < 0.01$.

if decreased mitochondrial oxidative enzyme expression in fast glycolytic fibers is indeed directly responsible for impaired exercise capacity under the CHF condition.

In fact, the deteriorated exercise capacity observed in this study occurred in the absence of a significant change in fiber type composition, confirmed by both fiber-typing analysis using indirect immunofluorescence (Table 1) and Western blot analysis for myosin heavy chain proteins (Figure 3A). These findings suggest that a shift from the slow fatigue-resistant oxidative fibers to the more fatigable glycolytic fibers is not always necessary for the development of exercise intolerance, which has also been noticed in other clinical studies.[16] Of course, our findings do not exclude the possibility that such a fiber type change in human patients with CHF contributes to deteriorated exercise capacity. Nevertheless, they do seem to be different from previous findings in humans and other species.[7,13–15] In addition to the possible species differences, one important factor to be considered is that the mice used in this study developed cardiac dysfunction rapidly[32] and had suffered from CHF for a short period of time (~3 to 4 weeks) compared with human CHF patients who usually have the cardiac conditions for years. Thus, the abnormalities that we observed in CSQ mice might represent the early stage of skeletal muscle abnormalities in CHF. Given the complexity and heterogeneity of CHF in humans, we do not expect a model to recapitulate all of the pathological changes in the skeletal muscle of CHF patients. Still, we believe this genetic model of CHF provides an excellent opportunity to reliably detect early skeletal muscle changes induced by CHF. Lack of certain pathological changes, such as a decrease percentage of slow oxidative fibers, allowed us to assess the contribution of other factors to the impaired physiological function in a whole animal setting.

Skeletal muscle atrophy is a prominent etiology of chronic diseases. Muscle wasting usually starts long before the appearance of clinical signs of overt cachexia. It has been well documented that noncachetic patients with CHF show reduced leg lean tissue compared with healthy patients,[45] suggesting that muscle wasting presents an initial pathological change for the clinical symptoms of the disease. Our findings in this study clearly demonstrate the prevalence of muscle wasting and structural deterioration in fast-twitch, glycolytic fibers as determined by normalized muscle weight (Table 1), fiber-specific measurement of the cross-sectional area of myofibers (Figure 4, A–D), morphological analysis by transmission electron microscopy (Figure 4, E and F; and Table 2), and mRNA expression of E3 ligases in the proteosome-dependent protein degradation pathway (Figure 5, A–D). These observations are consistent with and provide more comprehensive evidence to the previous findings that under the conditions of muscle atrophy fast glycolytic muscles are more prone to atrophic signals,[17–23] with exception to conditions of physiological or pathological disuse, in which slow oxidative fibers are more susceptible to the perturbation than fast glycolytic fibers.[46–48]

The involvement of the ubiquitin-proteasome pathway in muscle atrophy has been well established. Of particular interest was the identification of two genes, *MuRF1*

and *MAFbx/Atrogin-1*.[34,35] These genes encode E3 ubiquitin ligases[34] and have been shown to be up-regulated in various types of muscle atrophy.[34,35,38,49–51] More importantly, overexpression of MuRF1 protein results in the disruption of contractile protein,[52] and mice null for the *MuRF1* (*MuRF1*$^{-/-}$) or the *MAFbx/Atrogin-1* (*MAFbx/Atrogin-1*$^{-/-}$) gene have attenuated loss of muscle mass under the atrophic conditions compared with the WT littermates.[34] Enhanced expression of *MuRF1* and/or *MAFbx/Atrogin-1* mRNA now serves as a marker of skeletal muscle atrophy. Using RT-PCR analysis, we now have obtained evidence at the mRNA levels that further supports the aforementioned findings of manifested skeletal abnormalities in fast glycolytic myofibers. We observed a significant induction of *MAFbx/Atrogin-1* mRNA in fast glycolytic white vastus lateralis muscle, but not in slow oxidative soleus muscle, in CSQ mice. This was further supported by our finding that there was a more dramatic induction of *MAFbx/Atrogin-1* in white vastus lateralis muscle than in soleus muscle and no induction of *MuRF1* mRNA in soleus muscle, but significant induction in white vastus lateralis muscle *in vivo* after a single intraperitoneal injection of TNF-α or LPS (Figure 5, C and D). It seems that the protection against muscle atrophy in slow oxidative muscle occurs not only under CHF condition but also under other pathological conditions for skeletal muscle atrophy.

An interesting finding in this study is that muscle atrophy developed in CSQ transgenic mice with CHF was associated with enhanced expression of *MAFbx/Atrogin-1* mRNA but not *MuRF1* mRNA. It has been speculated that *MuRF1* and *MAFbx/Atrogin-1* mRNA expression under atrophic conditions are promoted via distinct signaling pathways. For example, enhanced expression of *MAFbx/Atrogin-1* mRNA has been shown to be mediated by the p38 mitogen-activated protein kinase pathway.[37] In transgenic mice with muscle-specific activation of the nuclear factor-κB pathway, muscle atrophy was induced along with enhanced expression of *MuRF1* mRNA, but not *MAFbx/Atrogin-1* mRNA.[53,54] The upstream signaling pathway responsible for the induced *MAFbx/Atrogin-1* mRNA expression in the current model of CHF remains to be ascertained. Delineation of signaling pathways in the development of skeletal muscle atrophy under different disease conditions will provide valuable information for the discovery of appropriate drug targets for treatment of this prevalent clinical etiology that affects virtually every patient with chronic diseases.

In summary, combinatory functional and analytical tests suggest that exercise intolerance can occur in the absence of significant fiber type switching in skeletal muscle, which has previously been speculated to play an important role in impaired exercise capacity in CHF patients. We have detected and compared fiber type-specific muscle atrophy, reduction of mitochondrial oxidative enzyme expression, vascular rarefaction, and enhanced muscle-specific E3 ubiquitin ligase mRNAs in skeletal muscles in a mouse model of CHF. The comprehensive biochemical, morphological, and transcriptional evidence strongly supports the view that CHF results in manifested abnormalities in fast-twitch, glycolytic fibers in skeletal muscle and that oxidative muscle phenotype provides a protection against pathological stimuli.

Acknowledgments

We thank Drs. R.S. Williams and H.A. Rockman and Ms. Mary Reedy for critical review of the manuscript; Ms. Jin Yan for careful proofreading; Dr. S.E. Miller and Mr. C.Z. Ireland for the excellent technical support; and Dr. H.A. Rockman for the generous gift of CSQ transgenic mice.

References

1. Chati Z, Zannad F, Michel C, Lherbier B, Mertes PM, Escanye JM, Ribout C, Robert J, Villemot JP, Aliot E: Skeletal muscle phosphate metabolism abnormalities in volume-overload experimental heart failure. Am J Physiol 1994, 267:H2186–H2192
2. Clark AL, Poole-Wilson PA, Coats AJ: Exercise limitation in chronic heart failure: central role of the periphery. J Am Coll Cardiol 1996, 28:1092–1102
3. Clark AL, Sparrow JL, Coats AJ: Muscle fatigue and dyspnoea in chronic heart failure: two sides of the same coin. Eur Heart J 1995, 16:49–52
4. Drexler H, Riede U, Munzel T, Konig H, Funke E, Just H: Alterations of skeletal muscle in chronic heart failure. Circulation 1992, 85:1751–1759
5. Harrington D, Coats AJ: Skeletal muscle abnormalities and evidence for their role in symptom generation in chronic heart failure. Eur Heart J 1997, 18:1865–1872
6. Minotti JR, Christoph I, Oka R, Weiner MW, Wells L, Massie BM: Impaired skeletal muscle function in patients with congestive heart failure. Relationship to systemic exercise performance. J Clin Invest 1991, 88:2077–2082
7. Caforio AL, Rossi B, Risaliti R, Siciliano G, Marchetti A, Angelini C, Crea F, Mariani M, Muratorio A: Type 1 fiber abnormalities in skeletal muscle of patients with hypertrophic and dilated cardiomyopathy: evidence of subclinical myogenic myopathy. J Am Coll Cardiol 1989, 14:1464–1473
8. Sullivan MJ, Duscha BD, Klitgaard H, Kraus WE, Cobb FR, Saltin B: Altered expression of myosin heavy chain in human skeletal muscle in chronic heart failure. Med Sci Sports Exerc 1997, 29:860–866
9. Sullivan MJ, Green HJ, Cobb FR: Skeletal muscle biochemistry and histology in ambulatory patients with long-term heart failure. Circulation 1990, 81:518–527
10. Reiken S, Lacampagne A, Zhou H, Kherani A, Lehnart SE, Ward C, Huang F, Gaburjakova M, Gaburjakova J, Rosemblit N, Warren MS, He KL, Yi GH, Wang J, Burkhoff D, Vassort G, Marks AR: PKA phosphorylation activates the calcium release channel (ryanodine receptor) in skeletal muscle: defective regulation in heart failure. J Cell Biol 2003, 160:919–928
11. Lipkin DP, Jones DA, Round JM, Poole-Wilson PA: Abnormalities of skeletal muscle in patients with chronic heart failure. Int J Cardiol 1988, 18:187–195
12. Schaufelberger M, Eriksson BO, Grimby G, Held P, Swedberg K: Skeletal muscle fiber composition and capillarization in patients with chronic heart failure: relation to exercise capacity and central hemodynamics. J Card Fail 1995, 1:267–272
13. Dalla Libera L, Ravara B, Angelini A, Rossini K, Sandri M, Thiene G, Battista Ambrosio G, Vescovo G: Beneficial effects on skeletal muscle of the angiotensin II type 1 receptor blocker irbesartan in experimental heart failure. Circulation 2001, 103:2195–2200
14. Vescovo G, Zennaro R, Sandri M, Carraro U, Leprotti C, Ceconi C, Ambrosio GB, Dalla Libera L: Apoptosis of skeletal muscle myofibers and interstitial cells in experimental heart failure. J Mol Cell Cardiol 1998, 30:2449–2459
15. Vescovo G, Dalla Libera L, Serafini F, Leprotti C, Facchin L, Volterrani M, Ceconi C, Ambrosio GB: Improved exercise tolerance after losartan and enalapril in heart failure: correlation with changes in skeletal

muscle myosin heavy chain composition. Circulation 1998, 98:1742–1749
16. Magnusson G, Gordon A, Kaijser L, Sylven C, Isberg B, Karpakka J, Saltin B: High intensity knee extensor training, in patients with chronic heart failure. Major skeletal muscle improvement. Eur Heart J 1996, 17:1048–1055
17. Fernández-Solá J, Sacanella E, Estruch R, Nicolas JM, Grau JM, Urbano-Marquez A: Significance of type II fiber atrophy in chronic alcoholic myopathy. J Neurol Sci 1995, 130:69–76
18. Reilly ME, Erylmaz EI, Amir A, Peters TJ, Preedy VR: Skeletal muscle ribonuclease activities in chronically ethanol-treated rats. Alcohol Clin Exp Res 1998, 22:876–883
19. Shah AJ, Sahgal V, Quintanilla AP, Subramani V, Singh H, Hughes R: Muscle in chronic uremia—a histochemical and morphometric study of human quadriceps muscle biopsies. Clin Neuropathol 1983, 2:83–89
20. Medina-Sanchez M, Rodriguez-Sanchez C, Vega-Alvarez JA, Menedez-Pelaez A, Perez-Casas A: Proximal skeletal muscle alterations in streptozotocin-diabetic rats: a histochemical and morphometric analysis. Am J Anat 1991, 191:48–56
21. Butori C, Desnuelle C, Hofman P, Paquis V, Durant J, Carles M, Pesce A, Michiels JF: Muscular involvement in the course of AIDS. Anatomoclinical study of 17 cases. Ann Pathol 1995, 15:424–430
22. Minnaard R, Drost MR, Wagenmakers AJ, van Kranenburg GP, Kuipers H, Hesselink MK: Skeletal muscle wasting and contractile performance in septic rats. Muscle Nerve 2005, 31:339–348
23. Smith PF, Eydelloth RS, Grossman SJ, Stubbs RJ, Schwartz MS, Germershausen JI, Vyas KP, Kari PH, MacDonald JS: HMG-CoA reductase inhibitor-induced myopathy in the rat: cyclosporine A interaction and mechanism studies. J Pharmacol Exp Ther 1991, 257:1225–1235
24. Jones LR, Suzuki YJ, Wang W, Kobayashi YM, Ramesh V, Franzini-Armstrong C, Cleemann L, Morad M: Regulation of Ca2+ signaling in transgenic mouse cardiac myocytes overexpressing calsequestrin. J Clin Invest 1998, 101:1385–1393
25. Cho MC, Rapacciuolo A, Koch WJ, Kobayashi Y, Jones LR, Rockman HA: Defective beta-adrenergic receptor signaling precedes the development of dilated cardiomyopathy in transgenic mice with calsequestrin overexpression. J Biol Chem 1999, 274:22251–22256
26. Tanaka N, Dalton N, Mao L, Rockman HA, Peterson KL, Gottshall KR, Hunter JJ, Chien KR, Ross Jr J: Transthoracic echocardiography in models of cardiac disease in the mouse. Circulation 1996, 94:1109–1117
27. Rapacciuolo A, Esposito G, Caron K, Mao L, Thomas SA, Rockman HA: Important role of endogenous norepinephrine and epinephrine in the development of in vivo pressure-overload cardiac hypertrophy. J Am Coll Cardiol 2001, 38:876–882
28. Akimoto T, Ribar TJ, Williams RS, Yan Z: Skeletal muscle adaptation in response to voluntary running in Ca2+/calmodulin-dependent protein kinase IV (CaMKIV) deficient mice. Am J Physiol 2004, 287:C1311–C1319
29. Miller SE, Howell DN: Viral infections in the acquired immunodeficiency syndrome. J Electron Microsc Tech 1988, 8:41–78
30. Yan Z, Choi S, Liu X, Zhang M, Schageman JJ, Lee SY, Hart R, Lin L, Thurmond FA, Williams RS: Highly coordinated gene regulation in mouse skeletal muscle regeneration. J Biol Chem 2003, 278:8826–8836
31. Riccio A, Medhurst AD, Mattei C, Kelsell RE, Calver AR, Randall AD, Benham CD, Pangalos MN: mRNA distribution analysis of human TRPC family in CNS and peripheral tissues. Brain Res Mol Brain Res 2002, 109:95–104
32. Suzuki M, Carlson KM, Marchuk DA, Rockman HA: Genetic modifier loci affecting survival and cardiac function in murine dilated cardiomyopathy. Circulation 2002, 105:1824–1829
33. Waters RE, Rotevatn S, Li P, Annex BH, Yan Z: Voluntary running induces fiber type-specific angiogenesis in mouse skeletal muscle. Am J Physiol 2004, 287:C1342–C1348
34. Bodine SC, Latres E, Baumhueter S, Lai VK, Nunez L, Clarke BA, Poueymirou WT, Panaro FJ, Na E, Dharmarajan K, Pan ZQ, Valenzuela DM, DeChiara TM, Stitt TN, Yancopoulos GD, Glass DJ: Identification of ubiquitin ligases required for skeletal muscle atrophy. Science 2001, 294:1704–1708
35. Gomes MD, Lecker SH, Jagoe RT, Navon A, Goldberg AL: Atrogin-1, a muscle-specific F-box protein highly expressed during muscle atrophy. Proc Natl Acad Sci USA 2001, 98:14440–14445
36. Lecker SH, Jagoe RT, Gilbert A, Gomes M, Baracos V, Bailey J, Price SR, Mitch WE, Goldberg AL: Multiple types of skeletal muscle atrophy involve a common program of changes in gene expression. FASEB J 2004, 18:39–51
37. Li YP, Chen Y, John J, Moylan J, Jin B, Mann DL, Reid MB: TNF-alpha acts via p38 MAPK to stimulate expression of the ubiquitin ligase atrogin1/MAFbx in skeletal muscle. FASEB J 2005, 19:362–370
38. Dehoux MJ, van Beneden RP, Fernandez-Celemin L, Lause PL, Thissen JP: Induction of MafBx and Murf ubiquitin ligase mRNAs in rat skeletal muscle after LPS injection. FEBS Lett 2003, 544:214–217
39. Burniston JG, Saini A, Tan LB, Goldspink DF: Angiotensin II induces apoptosis in vivo in skeletal, as well as cardiac, muscle of the rat. Exp Physiol 2005, 90:755–761
40. Burniston JG, Saini A, Tan LB, Goldspink DF: Aldosterone induces myocyte apoptosis in the heart and skeletal muscles of rats in vivo. J Mol Cell Cardiol 2005, 39:395–399
41. Duscha BD, Annex BH, Keteyian SJ, Green HJ, Sullivan MJ, Samsa GP, Brawner CA, Schachat FH, Kraus WE: Differences in skeletal muscle between men and women with chronic heart failure. J Appl Physiol 2001, 90:280–286
42. Nusz DJ, White DC, Dai Q, Pippen AM, Thompson MA, Walton GB, Parsa CJ, Koch WJ, Annex BH: Vascular rarefaction in peripheral skeletal muscle after experimental heart failure. Am J Physiol 2003, 285:H1554–H1562
43. De Sousa E, Veksler V, Bigard X, Mateo P, Ventura-Clapier R: Heart failure affects mitochondrial but not myofibrillar intrinsic properties of skeletal muscle. Circulation 2000, 102:1847–1853
44. Keteyian SJ, Duscha BD, Brawner CA, Green HJ, Marks CR, Schachat FH, Annex BH, Kraus WE: Differential effects of exercise training in men and women with chronic heart failure. Am Heart J 2003, 145:912–918
45. Anker SD, Ponikowski P, Varney S, Chua TP, Clark AL, Webb-Peploe KM, Harrington D, Kox WJ, Poole-Wilson PA, Coats AJ: Wasting as independent risk factor for mortality in chronic heart failure. Lancet 1997, 349:1050–1053
46. Riley DA, Bain JL, Thompson JL, Fitts RH, Widrick JJ, Trappe SW, Trappe TA, Costill DL: Disproportionate loss of thin filaments in human soleus muscle after 17-day bed rest. Muscle Nerve 1998, 21:1280–1289
47. Roy RR, Bodine SC, Pierotti DJ, Kim JA, Talmadge RJ, Barkhoudarian G, Fanton JW, Koslovskaya I, Edgerton VR: Fiber size and myosin phenotypes of selected Rhesus hindlimb muscles after a 14-day spaceflight. J Gravit Physiol 1999, 6:55–62
48. Squier M, Chalk C, Hilton-Jones D, Mills KR, Newsom-Davis J: Type 2 fiber predominance in Lambert-Eaton myasthenic syndrome. Muscle Nerve 1991, 14:625–632
49. DeRuisseau KC, Kavazis AN, Deering MA, Falk DJ, Van Gammeren D, Yimlamai T, Ordway GA, Powers SK: Mechanical ventilation induces alterations of the ubiquitin-proteasome pathway in the diaphragm. J Appl Physiol 2005, 98:1314–1321
50. Li YP, Chen Y, Li AS, Reid MB: Hydrogen peroxide stimulates ubiquitin-conjugating activity and expression of genes for specific E2 and E3 proteins in skeletal muscle myotubes. Am J Physiol 2003, 285:C806–C812
51. Latres E, Amini AR, Amini AA, Griffiths J, Martin FJ, Wei Y, Lin HC, Yancopoulos GD, Glass DJ: Insulin-like growth factor-1 (IGF-1) inversely regulates atrophy-induced genes via the phosphatidylinositol 3-kinase/Akt/mammalian target of rapamycin (PI3K/Akt/mTOR) pathway. J Biol Chem 2005, 280:2737–2744
52. McElhinny AS, Kakinuma K, Sorimachi H, Labeit S, Gregorio CC: Muscle-specific RING finger-1 interacts with titin to regulate sarcomeric M-line and thick filament structure and may have nuclear functions via its interaction with glucocorticoid modulatory element binding protein-1. J Cell Biol 2002, 157:125–136
53. Cai D, Frantz JD, Tawa Jr NE, Melendez PA, Oh BC, Lidov HG, Hasselgren PO, Frontera WR, Lee J, Glass DJ, Shoelson SE: IKKbeta/NF-kappaB activation causes severe muscle wasting in mice. Cell 2004, 119:285–298
54. Kamei Y, Miura S, Suzuki M, Kai Y, Mizukami J, Taniguchi T, Mochida K, Hata T, Matsuda J, Aburatani H, Nishino I, Ezaki O: Skeletal muscle FOXO1 (FKHR) transgenic mice have less skeletal muscle mass, down-regulated type I (slow twitch/red muscle) fiber genes, and impaired glycemic control. J Biol Chem 2004, 279:41114–41123